

# Rayleigh Damping Modelling to Assess Viscous Behaviour in Actuated Breast Tissue

Jessica. L Fitzjohn\* Cong Zhou\* J. Geoffrey Chase\*  
Zane Ormsby\*\* Marcus Hagggers\*\*

\* *Department of Mechanical Engineering, Centre for Bio-engineering,  
University of Canterbury, Christchurch, New Zealand (e-mail:  
jessica.fitzjohn@pg.canterbury.ac.nz, cong.zhou@canterbury.ac.nz,  
geoff.chase@canterbury.ac.nz)*

\*\* *Tiro Medical, Christchurch, New Zealand (e-mail:  
zane.ormsby@tiromedical.com, marcus.hagggers@tiromedical.com)*

---

## Abstract:

Breast cancer is a significant health problem worldwide. Emerging non-invasive methods assess tumor presence by its impact on breast tissue mechanics. This paper outlines a method to identify equivalent viscous damping in breast tissue and fit a model based on the Rayleigh damping (RD) model. Surface motion information of actuated breast tissue was captured using the Digital Image Elasto Tomography (DIET) system. The viscous damping was calculated for over 14,000 reference points using an ellipse fitted to the force-displacement hysteresis loop response data to calculate work done. A damping model based on RD is suggested and fit to median filtered data of viscous damping constant plotted against the major ellipse axis. This successfully described the trend for all 29 breasts (14 cancerous, 15 healthy) with average  $R^2$  values ranging from 0.79-0.88. One model coefficient, 'a', proportional to local mass, showed reasonable consistency among the subjects and decreased with increasing frequency. No significant difference in this 'a' coefficient between healthy and cancerous breasts showed indication of diagnostic potential. However, consistent values across all breasts suggest it is a fundamental tissue property. Further suggestions to normalise the major axis by frequency demonstrate the potential for the model to be developed to describe viscous behaviour of breast tissue in the form of storage and loss modulus.

*Keywords:* Tumor detection, Breast cancer, Viscous damping, Digital Imaging, DIET

---

## 1. INTRODUCTION

Breast cancer is the most frequent cancer and leading cause of cancer deaths in women worldwide (van den Ende et al., 2017; Lotz et al., 2011b). More than 1 million women are diagnosed each year, with approximately 400,000 mortalities (Coughlin and Ekwueme, 2009). Five year survival rates can increase to over 95% with early detection, due to increased treatment options (Heywang-Kbrunner et al., 2011; Jemal et al., 2011), demonstrating the need for effective, high compliance breast cancer screening programs.

X-ray mammography is currently the standard technique used for breast cancer screening. It involves painful breast compression and radiation exposure, limiting the safe age bracket for screening and leading to poor compliance (Fazel et al., 2009; van den Ende et al., 2017). Sensitivity can be low due to the small variation (5-10%) in radio density between healthy and cancerous breast tissue leading to false positives (Elmore et al., 2002; Hina Muhammad Ismail\* et al., 2017). Limited availability of mammography screening programs in developing countries and rural areas exist due to high cost and limited access to radiology clinics. These issues outline the need for breast cancer

screening to be affordable and easy to implement in all areas.

Digital Image Elasto Tomography (DIET) (Peters et al., 2004, 2008, 2005; Lotz et al., 2011a; Kashif, 2013) is a non-invasive alternative breast cancer screening approach, which utilizes the significant contrast in elastic properties (400-1000%) of healthy and cancerous tissue. The DIET system involves a mechanical actuator, which induces a steady state sinusoidal vibration in the breast while surrounding cameras capture images of the breast surface motion. These images are analysed using surface volume and optical flow techniques, resulting in displacement data for over 14,000 reference points on the breast surface.

The DIET system is portable and affordable and the test itself much more comfortable than a mammogram. Because it is non-invasive is it also suitable for all ages. Analysis of the surface motion data has so far yielded reasonable diagnostic success including a study on hysteresis loop analysis (HLA) (Zhou et al., 2018). However, the HLA method was tested using silicone phantoms with homogeneous properties and was not validated using more complex clinical data.

This paper suggests a model based on the Rayleigh damping (RD) model to describe viscous damping behaviour in breast tissue. The goal is to assess damping properties for diagnostic potential and physiological insight. It shows how this model consistently fits the curve shape of the equivalent viscous damping constant across a total of 29 breasts (14 cancerous, 15 healthy).

## 2. METHOD

### 2.1 Clinical Data

18 women were recruited to undergo a clinical trial at Canterbury Breast Care (Christchurch, NZ) using a prototype DIET system. Ethics approval for the experimental tests, data collection, and analysis of this data was granted by the NZ National Health and Disability Ethics Committee, South Island Regional Committee.

Of the 18 women tested, 15 had a tumor in one breast, one had a tumor in both breasts and two had both breasts healthy. Displacement data was obtained by Tiro Medical, a New Zealand based medical company, at a range of available testing frequencies. Some subjects had insufficient data for all input frequencies. These subjects were excluded, leading to a total of 14 cancerous breasts and 15 healthy breasts analysed.

### 2.2 Viscous Damping in Breast Tissue

The 14,000 reference points on the breast surface were split into two halves. Healthy breasts were segmented consistently down the center, cancerous breasts were segmented to ensure the clinically specified tumor location, found via x-ray mammography, was contained in the centre of one half. The segmentation method is shown in Fig. 1. This simple segmentation allowed healthy and tumor segments within the cancerous breast to be clearly distinguished to determine any notable differences. In future analysis when the tumor location is unknown, arbitrary segmentation will occur with the possibility of an increased number of segments and changing of the segment reference plane to ensure the tumor location is eventually captured.

Each reference point on the breast surface was modelled as a viscous damper with viscous damping constant calculated using Equation (1):

$$C_{eq} = \frac{W_d}{\pi\omega X^2}. \quad (1)$$

Where  $W_d$  is the work done,  $\omega$  is the input frequency, and  $X$  is the response amplitude found from fitting a sine wave to the displacement-time data. The area of an ellipse fitted

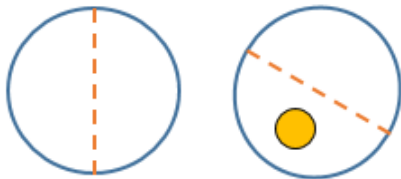


Fig. 1. Schematic of breast segmentation method showing tumor location

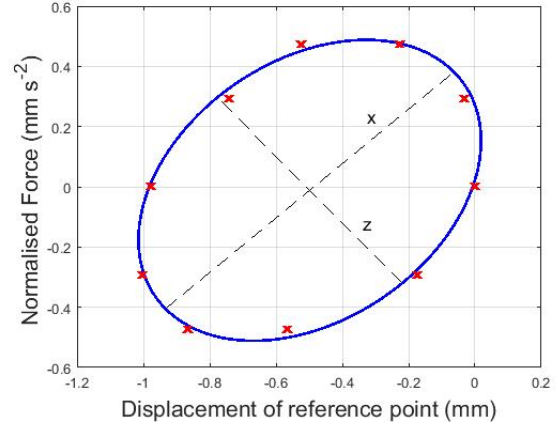


Fig. 2. Work done using area of ellipse

to the force-displacement plot of each reference point was used to find the work done by the actuator, as shown in Fig. 2, calculated:

$$W_d = \pi xz \quad (2)$$

Where  $x$  and  $z$  are the major and minor axes of the ellipse. The force used in the plot is the sinusoidal input force normalised by mass:

$$F = 0.5 \sin(\omega t) = 0.5 \sin(2\pi ft) \quad (3)$$

The damping constant was calculated for each reference point and plotted against the major axis of the ellipse for each separate segment.

### 2.3 Damping Model based on Rayleigh Damping

Rayleigh damping (RD) is commonly used to model structural damping in seismic analysis of buildings (Petrov et al., 2015). It is proportional to a linear combination of mass and stiffness, using a system damping matrix,  $C$ :

$$C = \mu M + \lambda K \quad (4)$$

Where  $\mu$  and  $\lambda$  are mass and stiffness proportional Rayleigh damping coefficients and  $M$  and  $K$  are the system mass and stiffness matrices. RD results in different damping ratios ( $\zeta$ ) for different response frequencies ( $\omega$ ):

$$\zeta = \frac{1}{2} \left( \frac{\mu}{\omega} + \lambda\omega \right) \quad (5)$$

A diagram of the general RD curve is shown in Fig. 3 showing the mass and stiffness contributions to the curve shape. The curve shape of Fig. 3 showed consistent resemblance to plots of equivalent viscous damping, compared to the major axis of the force-displacement ellipse, rather than frequency. This behaviour outlined the potential to infer viscous behaviour by implementing a similar model based on RD, defined:

$$C_{eq} = \frac{a}{x} + bx \quad (6)$$

Where  $a$  and  $b$  are breast and frequency specific coefficients and  $x$  is the length of the major axis of the force-displacement ellipse for each reference point. This model can be used to represent the viscous behaviour of breast tissue, which is consistent across a range of test subjects and has potential use in breast cancer diagnostics.

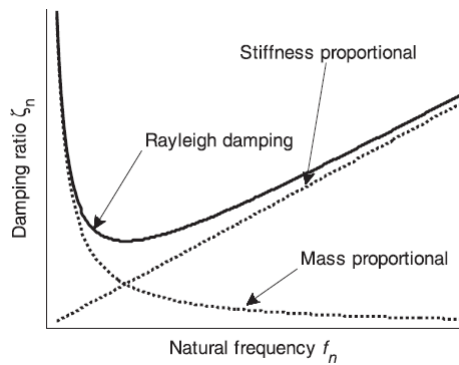


Fig. 3. Rayleigh damping curve showing mass and stiffness contributions

#### 2.4 Determining Model Coefficients using Median Filter

Prior to analysis large outliers were excluded by limiting  $x$  to between 0 and 0.1 and excluding overdamped points with equivalent viscous damping  $\zeta > 1$ . A median filter, with a window size of 10, was applied to the raw data to remove outliers and capture the trend represented by the bulk of the points.

The model in Equation (6) was then fit to the median filtered data to determine model coefficients 'a' and 'b' and  $R^2$  values. The 'a' coefficient is comparable to the mass proportional constant in RD, and is the focus of this paper. This value is expected to remain reasonably constant, as mass at a small, local point is hypothesised to be similar. Frequency dependence of both the 'a' coefficient and  $R^2$  values, to assess the success of the model fit, was assessed to test this hypothesis.

### 3. RESULTS AND DISCUSSION

#### 3.1 Median Filter and Model Fitting

Analysis of the distribution of viscous damping points in the breast showed reasonable consistency amongst all subjects with the 'back bone' of the curve comparable to the RD curve. Fig. 4 shows both the damping model fitted to the median filtered data (left) and the unfiltered data with damping model fit overlaid (right) for three randomly selected breast halves (2 cancerous, 1 healthy) at a given frequency of 38 Hz. The curve appears more dominated by the 'a' coefficient relative to mass, with smaller 'b' coefficients resulting in a flatter end of the curve compared to Rayleigh. It therefore follows a similar path to the mass proportional line shown in Fig. 3.

Fig. 4 shows fitting the damping curve to median filtered data is successful in capturing the curving trend of the majority of points. It also shows consistency in curve shape between breasts, which shows typical viscous behaviour has been captured.

#### 3.2 $R^2$ values

The  $R^2$  values fitted to the median filtered data demonstrates the damping model based on RD is applicable for assessing the equivalent viscous damping coefficients in

actuated breast tissue. The average  $R^2$  values are shown for each frequency in Table 1 for healthy and cancerous breasts. The  $R^2$  values for each half of the breast were very similar for both the healthy and tumor breasts and thus both sides were used to determine the averages.

The  $R^2$  values are acceptable for most subjects with only 7.8% of all  $R^2$  values less than 0.7 (4.5% healthy, 11.0% cancerous). Averages for cancerous and healthy breasts were similar. Thus, overall,  $R^2$  shows the model explains 79-88% of the observed points behaviour.

Table 1.  $R^2$  values for damping model fit of median filtered data in healthy and cancerous breasts

Frequency [Hz]	Average $R^2$ Healthy	Average $R^2$ Cancerous
20	0.79	0.79
23	0.83	0.86
26	0.87	0.81
29	0.85	0.83
32	0.86	0.82
35	0.88	0.82
38	0.88	0.83
41	0.88	0.79
44	0.85	0.81
47	0.85	0.80
50	0.86	0.85

#### 3.3 Frequency Dependence and Model Potential

The frequency dependence of the damping model fit was analysed for one patient, who had a tumor in one breast. Fig. 5 shows a clear increase in radius of curvature or 'a' coefficient with frequency in both the healthy and cancerous breast. The 'b' coefficient was also lower and more consistent in the healthy breast, while the cancerous breast showed some deviation from the typical flattening observed in Fig. 4 at some frequencies. This result outlines a possible diagnostic application for this model and further analysis of the 'b' coefficient values should be pursued.

Fig. 6 shows the frequency dependence of coefficient 'a' for all subjects in healthy and cancerous breasts. This shows reasonable consistency in values with most points within  $\pm 0.002$ . It also demonstrates an overall decreasing trend of 'a' coefficient values with frequency. This coefficient had little difference between healthy and cancerous breasts and did not show diagnostic potential, indicating it captures a fundamental tissue property common to all breasts.

#### 3.4 Model Potential

While analysis of the 'a' coefficient did not demonstrate diagnostic capability, the model itself and the consistency of the fit for all breasts analysed, shows potential to relate these coefficients to viscous properties of the breast. The vibration for each reference point can be represented by a single degree of freedom (SDOF) oscillator. For calculating RD in a steady state, SDOF system the mass and stiffness proportional damping constants can be reduced to:

$$\mu = \zeta \omega \quad (7)$$

$$\lambda = \frac{\zeta}{\omega} \quad (8)$$

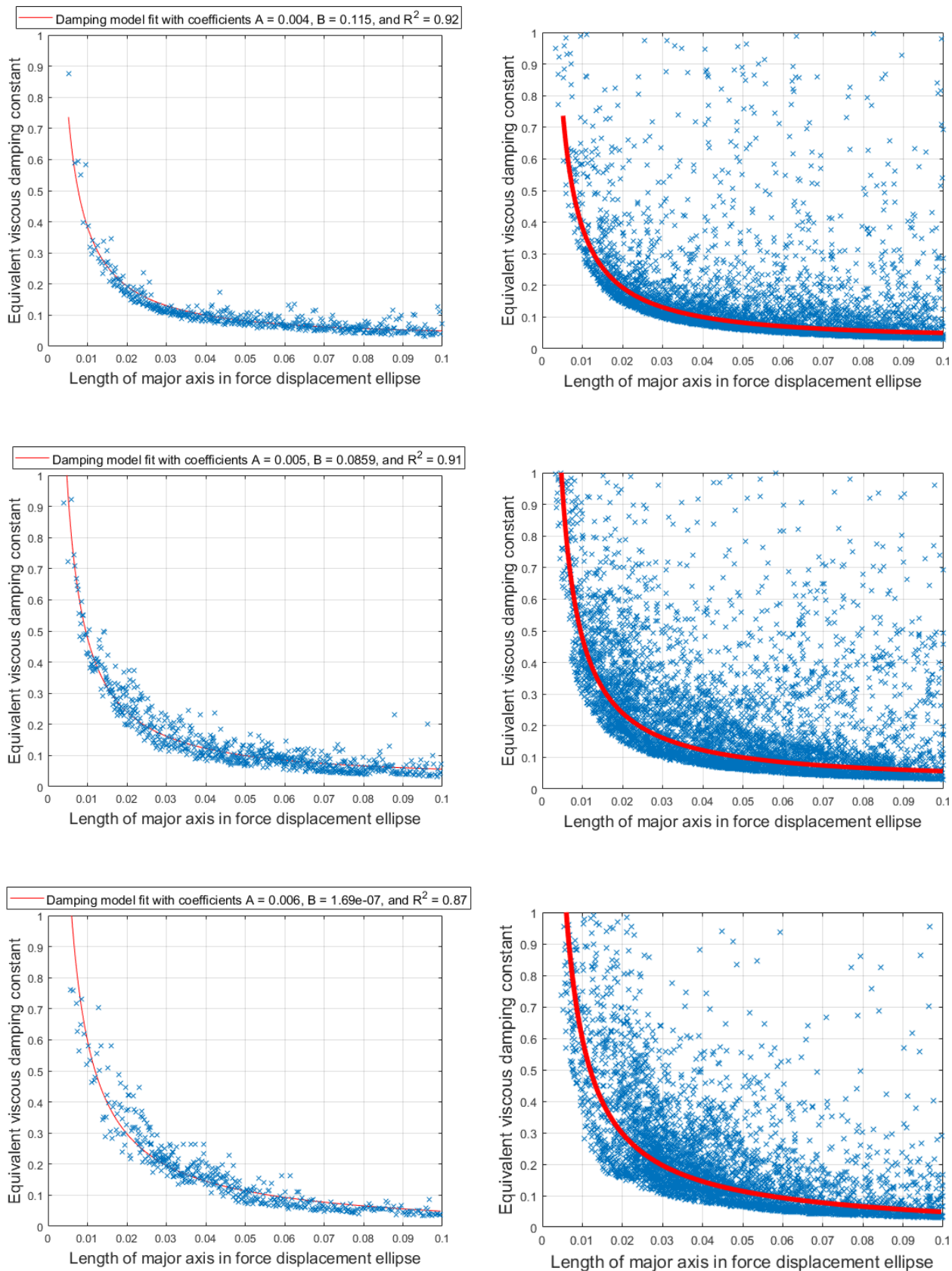


Fig. 4. Damping model fit to median filtered data (left) and unfiltered data (right) for input frequency = 38 Hz for three randomly selected breasts.

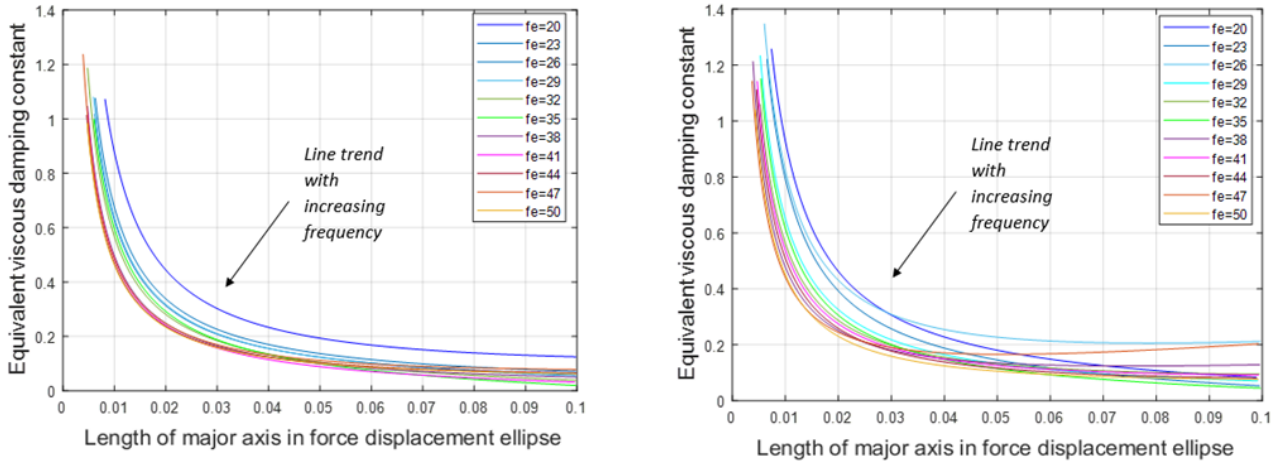


Fig. 5. Frequency dependence of damping model fit for one patient in healthy (left) and cancerous (right) breasts

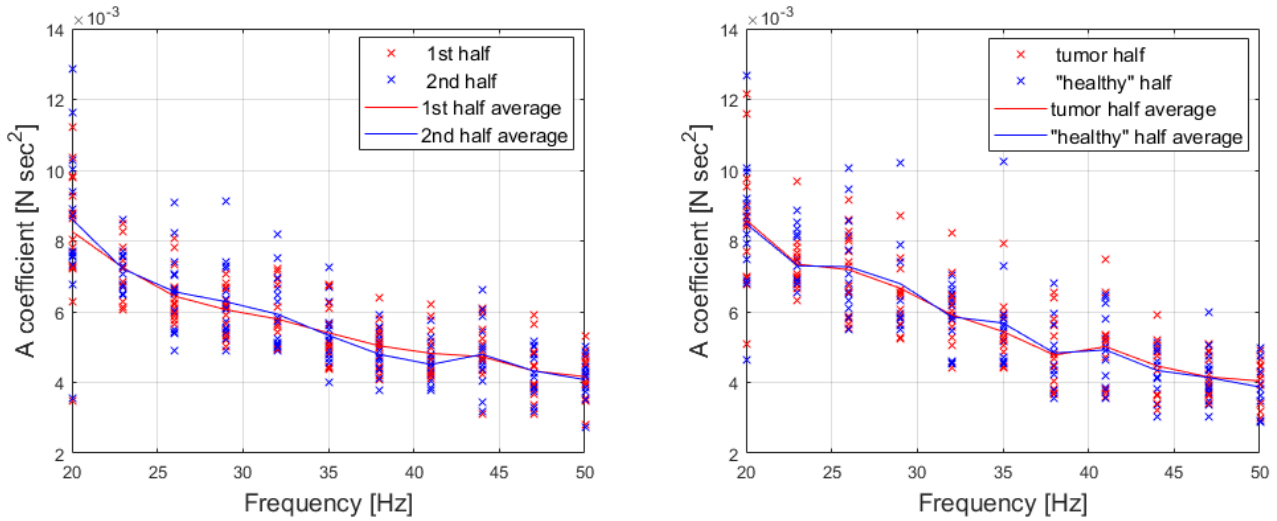


Fig. 6. Frequency dependence of damping model 'a' coefficient in healthy (left) and cancerous (right) breasts

Providing we assume the following:

- Mass is constant for each reference point
- Each reference point has non-linear response with an equivalent frequency  $\omega(i)$

Equation (4) can be transformed into:

$$C = \zeta m \omega + \zeta \frac{k}{\omega} \quad (9)$$

If we replace  $\omega$  with  $(x\omega)/x$ , where  $x$  is the length of the major axis of the ellipse used in the damping model, the equation becomes:

$$C = \zeta m \frac{x}{\omega} + \zeta \frac{k x}{x \omega} \quad (10)$$

If the current  $x$  in the damping model (Equation (6)) is normalised by frequency, changing to  $x/\omega$ , the new model is:

$$C = a_2 \frac{\omega}{x} + b_2 \frac{x}{\omega} \quad (11)$$

This normalisation will only effect the scale of the x-axis and will have no effect on the shape. It would also mean the

observed frequency dependence of 'a' would be accounted for in the new model. The new 'a<sub>2</sub>' and 'b<sub>2</sub>' coefficients would be described:

$$a_2 = \zeta m x \quad (12)$$

$$b_2 = \zeta \frac{k}{x} \quad (13)$$

This approach would give the 'a<sub>2</sub>' and 'b<sub>2</sub>' coefficients units of [Ns<sup>2</sup>] and [N/m/m], respectively. The unit of 'b<sub>2</sub>', N/m/m, is the unit of both storage and loss modulus, which describe the elastic and viscous portions of a material, respectively. Assessment of this coefficient, combined with the phase lag between stress and strain, could be used to infer visco-elastic properties of breast tissue simultaneously, potentially yielding new diagnostics and insight.

#### 4. CONCLUSION

While this method does not directly provide a diagnostic tool it provides a model, which consistently describes viscous damping in breast tissue for a range of subjects.

The mass based 'a' coefficient captures a fundamental, frequency dependent tissue property providing novel insight into breast tissue properties. Calculations demonstrated development of this model to include normalisation based on frequency and direct coefficient analysis could lead to viscous information regarding storage and loss modulus.

## 5. ACKNOWLEDGEMENTS

The authors acknowledge the support of Tiro Medical Ltd, Dr Richard Annand at Canterbury BreastCare and NZ National Science Challenge 7, Science for Technological Innovation (SfTI) as funded by the NZ Ministry for Business, Innovation and Enterprise.

## REFERENCES

- Coughlin, S. S., Ekwueme, D. U., 2009. Breast cancer as a global health concern. *Cancer epidemiology* 33 (5), 315–318.
- Elmore, J. G., Miglioretti, D. L., Reisch, L. M., Barton, M. B., Kreuter, W., Christiansen, C. L., Fletcher, S. W., 2002. Screening mammograms by community radiologists: variability in false-positive rates. *Journal of the National Cancer Institute* 94 (18), 1373–1380.
- Fazel, R., Krumholz, H. M., Wang, Y., Ross, J. S., Chen, J., Ting, H. H., Shah, N. D., Nasir, K., Einstein, A. J., Nallamothu, B. K., 2009. Exposure to low-dose ionizing radiation from medical imaging procedures. *New England Journal of Medicine* 361 (9), 849–857.
- Heywang-Kbrunner, S. H., Hacker, A., Sedlacek, S., 2011. Advantages and Disadvantages of Mammography Screening. *Breast Care* 6 (3), 2–2.
- Hina Muhammad Ismail\*, Christopher G. Pretty, Matthew K. Signal, Marcus Haggars and J. Geoffrey Chase, 2017. Attributes, Performance, and Gaps in Current & Emerging Breast Cancer Screening Technologies. *Current Medical Imaging Reviews* 13, 1–10.
- Jemal, A., Bray, F., Center, M. M., Ferlay, J., Ward, E., Forman, D., 2011. Global cancer statistics. *CA: a cancer journal for clinicians* 61 (2), 69–90.
- Kashif, A. S., 2013. Imaging technology for digital image based motion detection in the DIET breast cancer screening system. Ph.D. thesis, University of Canterbury.
- Lotz, T., Kashif, A., Feng, S., Biret, P., Denais, Y., Lottin, D., Maillard, L., Tirschler, T., Chase, J. G., 2011a. A clinical prototype of the digital image elasto tomography breast cancer screening system. *IEEE*, pp. 1–4.
- Lotz, T., Muller, N., Hann, C. E., Chase, J. G., Feb. 2011b. Minimal elastographic modeling of breast cancer for model based tumour detection in a Digital Image Elasto Tomography (DIET) System.
- Peters, A., Chase, J. G., Van Houten, E. E., 2008. Digital image elasto-tomography: combinatorial and hybrid optimization algorithms for shape-based elastic property reconstruction. *IEEE transactions on biomedical engineering* 55 (11), 2575–2583.
- Peters, A., Milsant, A., Rouz, J., Ray, L., Chase, J. G., Houten, E. E. W. V., 2004. Digital image-based elasto-tomography: Proof of concept studies for surface based mechanical property reconstruction. *JSME International Journal Series C Mechanical Systems, Machine Elements and Manufacturing* 47 (4), 1117–1123.
- Peters, A., Wortmann, S., Elliot, R., Staiger, M., Chase, J., Van Houten, E. E., 2005. Digital Image-based Elasto-Tomography: First experiments in surface based mechanical property estimation of gelatine phantoms. *JSME International Journal* 48 (4), 562–569.
- Petrov, A. Y., Docherty, P. D., Sellier, M., Chase, J. G., Jan. 2015. Multi-frequency Rayleigh damped elastography: in silico studies. *Medical Engineering & Physics* 37 (1), 55–67.
- van den Ende, C., Oordt-Speets, A. M., Vroling, H., van Agt, H. M. E., Oct. 2017. Benefits and harms of breast cancer screening with mammography in women aged 40-49 years: A systematic review: Breast Cancer Screening in Women Aged 40-49 years. *International Journal of Cancer* 141 (7), 1295–1306.
- Zhou, C., Chase, J. G., Ismail, H., Signal, M. K., Haggars, M., Rodgers, G. W., Pretty, C., 2018. Silicone phantom validation of breast cancer tumor detection using nominal stiffness identification in digital imaging elasto-tomography (DIET). *Biomedical Signal Processing and Control* 39, 435–447.